Quaternary Science Reviews 258 (2021) 106866

Contents lists available at ScienceDirect

Quaternary Science Reviews

journal homepage: www.elsevier.com/locate/quascirev

30,000 years of landscape and vegetation dynamics in a mid-elevation Andean valley

C.N.H. McMichael [a, *], N.H. Witteveen [a], S. Scholz [a], M. Zwier [b, 1], M.A. Prins [b], B.C. Lougheed [c], P. Mothes [d], W.D. Gosling [a]

[a] Department of Ecosystem and Landscape Dynamics, Institute for Biodiversity and Ecosystem Dynamics, University of Amsterdam, Science Park 904, 1098 GE, Amsterdam, Netherlands
[b] Department of Earth Sciences, Vrije Universiteit, De Boelelaan 1085, 1081 HV, Amsterdam, Netherlands
[c] Department of Earth Sciences, Uppsala University, Villavägen 16, 752 36, Uppsala, Sweden
[d] Instituto Geofísico, Escuela Politécnica Nacional, Casilla, 1701-2759, Quito, Ecuador

ARTICLE INFO

Article history:
Received 8 June 2020
Received in revised form
24 January 2021
Accepted 24 February 2021
Available online 19 March 2021

Handling Editor: I. Hendy

Keywords:
Charcoal
Fire
Eastern Andes
Holocene
Palms
Phytoliths
Pleistocene
River dynamics

ABSTRACT

The mid-elevation settings of the Andes are important biodiversity hotspots, yet little is known of their long-term ecology or environmental change. Here, we assess 30,000 years of landscape and vegetation dynamics on an alluvial terrace located in a mid-elevation valley of the Ecuadorian Andes (Campo Libre). We used loss-on-ignition and particle size analysis to reconstruct past river dynamics, charcoal analysis to reconstruct past fire regimes, and phytolith analysis to reconstruct vegetation change through time. Our results show that Campo Libre was a part of the active floodplain system of the Quijos River until 18,000 cal yr BP. The biggest vegetation change in vegetation at Campo Libre occurred ca. 13,000 cal yr BP, when the site warmed and dried, transforming the swampy alluvial terrace into a palm forest. As Holocene precipitation increased, the site transformed back into a swamp around 7500 cal yr BP, and it remained that way until maize agriculture began around 4600 cal yr BP. Local and regional fires were absent from the system until regional fires were detected ca. 3300 cal yr BP. By ca. 2700 cal yr BP, maize cultivation became frequent and regular. Climate, tectonic activity, and the human history have shaped the modern vegetation around Campo Libre, although during different periods of the Holocene. Our results demonstrate the ability of phytoliths to reconstruct vegetation change through time, and show that the mid-elevation Andean valley systems were highly dynamic over the last 30,000 years.

© 2021 The Authors. Published by Elsevier Ltd. This is an open access article under the CC BY license (http://creativecommons.org/licenses/by/4.0/).

1. Introduction

The Eastern Andean Flank (EAF) in Ecuador is a biodiversity hotspot (Myers et al., 2000). Its steep elevational gradient, with the Amazonian rainforests at the lower end, and the páramo grasslands at the upper end, creates a large range of environmental conditions in relatively short geographical distance (ca. 120 km). Species richness is typically highest along this gradient between 1000 and 2000 m above sea level (masl) (Colwell, 2000; Rahbek, 1995; Terborgh, 1977; Jørgensen et al., 2011). These mid-elevation forests are also particularly threatened systems, both in terms of human pressures and climatic change (Cuesta et al., 2019; Myers et al., 2000; van Der Werff and Consiglio, 2004).

Mid-elevation Andean forests have also faced pressures of climatic change and human impacts in the past. Species have migrated up- and downslope in response to climate change on ecological and geological timescales (e.g., Bush et al., 2011; Groot et al., 2011; Hooghiemstra and Cleef, 1995). For example, during the last glacial period, species in Andean systems could live at much lower elevations than in the warmer climate of the current interglacial period (e.g. Liu and Colinvaux, 1985; Montoya et al., 2018). The deglaciation, or transition from the last glacial period to the current interglacial period (the Holocene), resulted in spatially variable climate and landscape changes that were abrupt and high-magnitude across South America (Clark et al., 2012).

In the Holocene (11,700 cal yr BP – present), temperature has remained relatively constant in the tropical Andes, though precipitation patterns have varied temporally and spatially (e.g., Bush

* Corresponding author. University of Amsterdam, 904 Science Park, 1098 GE, Amsterdam, Netherlands.
E-mail address: c.n.h.mcmichael@uva.nl (C.N.H. McMichael).
[1] Department of Biological Sciences and Bjerknes Centre for Climate Research, University of Bergen, Thormøhlensgate 53A, 5006 Bergen, Norway

https://doi.org/10.1016/j.quascirev.2021.106866
0277-3791/© 2021 The Authors. Published by Elsevier Ltd. This is an open access article under the CC BY license (http://creativecommons.org/licenses/by/4.0/).

and Gosling, 2012; Flantua et al., 2016). The most marked changes in overall precipitation occurred during the early and mid-Holocene, when the Andes and Amazon regions became drier (e.g. Bush and Gosling, 2012; Mayle and Power, 2008). Droughts during this period, as recorded in many lake sediment and stalagmite records, were generally time-transgressive and varied in intensity across geographic space (Bush et al., 2014). The speleothem record from Santiago cave on the lower slopes of the eastern Andes (Fig. 1) suggests that the period from 11,000 to 9000 cal yr BP was the driest time in the last 100,000 years (Mosblech et al., 2012). Shorter-term variations in climate, including changes in El Niño frequency and intensity, also occurred in the Neotropics and the Andes throughout the Holocene, and have intensified over the last several thousand years (Bustamante et al., 2016; Conroy et al., 2010; Moy et al., 2002; Riedinger et al., 2002).

People have occupied the Northern Andes since at least ca. 13,000 cal yr BP, with evidence for permanent settlements dating back to 7000 cal yr BP (e.g. Goldberg et al., 2016; Rademaker et al., 2014). Evidence of maize cultivation has also been found in both the high Andes and in Amazonia ca. 6000 cal yr BP (Athens et al., 2016; Bush et al., 1989, 2016). Human populations on the eastern Andes grew gradually through most of the Holocene, but then seemed to increase exponentially after ca. 5000 cal yr BP (Goldberg et al., 2016). Relatively little is known, however, about the past human history in mid-elevation forests compared with the Andean highlands above and the Amazonian lowlands below. Vegetation reconstructions using pollen analysis from lake sediment cores indicate a marked human presence in some mid-elevation forests (Åkesson et al., 2019; Bush et al., 2015; Loughlin et al., 2018b; Matthews-Bird et al., 2017; Raczka et al., 2019), while others lack evidence of human activity (Huisman et al., 2019; Schiferl et al., 2017).

Pollen is the most common proxy used in past vegetation reconstructions, but it degrades (oxidizes) in certain depositional environments. Pollen preserves best in deep anoxic lakes, which are rare in the mid-elevation areas of the Andes. Furthermore, pollen from many montane plant species can disperse over long distances. This input of both local and regional pollen into the lakes sediments can make interpretations of the vegetation composition and change through time complex (e.g. Hagemans et al., 2019; Urrego et al., 2011; Weng, 2005).

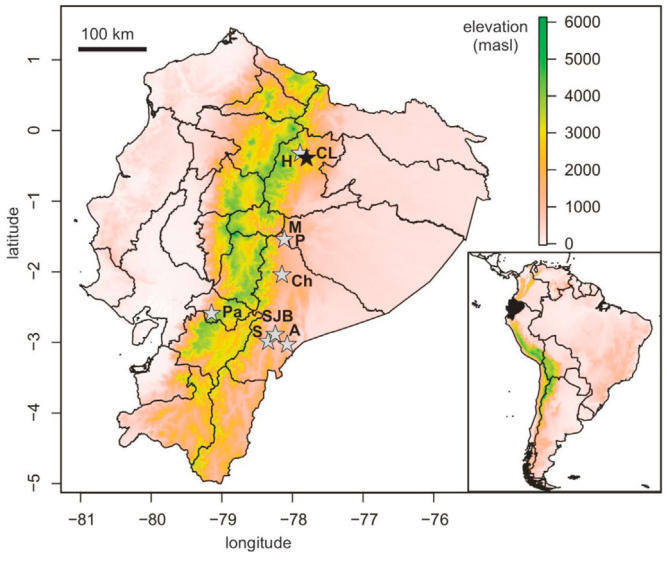

Fig. 1. Map of Ecuador showing Campo Libre (CL) and other sites mentioned in the text; sites are shown in relation to elevation. H = Huila (Loughlin et al., 2018b), M = Mera (Bush et al., 1990), SJB = San Juan Bosco (Bush et al., 1990), P = Pindo (Montoya et al., 2018), Ch = Lake Chimerella (Huisman et al., 2019), Pa = Laguna Pallcacocha (Moy et al., 2002), A = Lake Ayauch[i] (Bush et al., 1989), S = Santiago Cave speleothem (Mosblech et al., 2012).

Phytoliths are another proxy for vegetation commonly used in archaeological and paleoecological reconstructions (Piperno, 2006), and they preserve in many environments where pollen grains do not. Phytoliths are silica bodies produced in the structural and vegetative cells of many plants, and thus unlike pollen rarely disperse via the wind, and consequently reflect local patterns of vegetation (Piperno, 2006). They are also particularly sensitive to detecting human activities including cultivation, forest clearing, and forest management (e.g. McMichael et al., 2012; Piperno et al., 2019). Reconstructions using phytoliths in mid-elevation Andean forests are becoming more common (Bush et al., 1990; Colinvaux et al., 1996; Huisman et al., 2019a), and recent advances in the identification of Andean and Amazonian phytoliths (e.g., Huisman and Raczka, 2018; Morcote-Ríos and Bernal, 2016; Piperno et al., 2019) are now allowing for more taxonomically detailed vegetation reconstructions.

Here, we reconstruct ca. 30,000 years of fire, vegetation change, and human history in a mid-elevation setting in the Northern Andes (Ecuador) using phytolith and charcoal data. We place the vegetation data in the context of changes in the depositional environment through analysis of sediment particle size and loss-on-ignition. We also assess the watershed and floodplain configuration of our study system to interpret the vegetation change captured in our phytolith analysis. We compare our results with other reconstructions of past climate change and human activity to determine the relative role of climate and human drivers of change in hyper-diverse mid-elevation Andean forests.

2. Methods

2.1. Site and core description

Our study site is Campo Libre (S 00° 26.776′, W 77° 51.754’), which is currently a terrace overlooking the Quijos River, located on the Eastern Andean Flank (EAF) at 1800 m above sea level (masl) (Fig. 1). Campo Libre is located in the Subandean Zone, atop a terrace of the Cuyuja lava flow (210 ka) which was borne on Antisana Volcano, 30 km upslope (Hall et al., 2017), and located on the Eastern toe of the Cordillera Real mountain chain (de Berc et al., 2005). It lies between the towns of Baeza and San Francisco de Borja. The region has a mean annual temperature of 17.5–18.2 °C and annual precipitation amounts of 2220–2639 mm, with high rainfall throughout the year (monthly precipitation 144–298 mm; climate-data.org). The Rio Quijos valley is currently ca. 90 m lower in elevation, and ca. 1 km horizontal distance and due south from the Campo Libre core site. The current vegetation of the area around the Campo Libre core site is composed of a swampy (grassland) environment surrounded by lower montane rainforest. Pooideae (grasses), Bambusoideae (grasses) and Cyperaceae (sedges), with small, scattered forest patches compose the immediate area of the coring site. A few palms are also present within a 100–200 m from the site. Vegetation surveys were not conducted around the coring location, but several palm species occur in the region at elevations between 1900 and 2150 masl, including *Aiphanes verrucosa*, *Ceroxylon parvifrons*, *Chamaedorea pinnatifrons*, *Dictyocaryum lamarckianum*, *Euterpe precatoria*, *Geonoma densa*, *Geonoma orbignyana*, *Geonoma paradoxa*, *Prestoea acuminata* and *Wettinia aequatorialis* (Svenning et al., 2009).

In 2008, a 423-cm sediment core was retrieved from Campo Libre in seven sections (drives) with a Colinvaux-Vonhout piston-corer. The top three drives were collected with a 7-cm diameter

core tube, and the lower four were collected with a 5-cm diameter core tube. Once recovered, the drives were split and stored at 4 °C at the Open University (Milton Keynes, UK) and subsequently the University of Amsterdam.

2.2. Laboratory analysis

2.2.1. Radiocarbon dating

Six bulk sediment sub-samples, c. 1 cm^3 in volume, were extracted from the sediment core and sent to DirectAMS Laboratory (Seattle, Washington, USA) for radiocarbon (^{14}C) dating. Two other sub-samples, one bulk sediment and one woody plant sample, were analyzed at the ^{14}C facilities of the Tandem Laboratory, Uppsala University, Sweden. Radiocarbon dates were calibrated using the IntCal13 calibration curve (Reimer et al., 2013), and the calibrated ages were used to construct an age-depth model for the core using Bacon source code (Blaauw and Christen, 2011) for R (R Development Core Team, 2013).

2.2.2. Sediment characteristics

We extracted a total of 83 sub-samples (0.5 cm^3 each) for particle size analysis and 87 subsamples (0.5 cm^3 each) for loss-on-ignition (LOI) analysis from the sediment core. Sub-samples were extracted at 10 cm intervals throughout the entire core. We also extracted subsamples between 355 and 200 cm at 5 cm intervals, and 260-215 cm and 340-320 cm at 2 cm intervals.

Particle size analysis provided the percentage abundance of sediment particles in three size classes: <8 μm (clays), 8–63 μm (silts), and 63–2000 μm (sands). Samples were pre-treated according to Konert and Vandenberghe (1997). Organic material was removed by adding 5 ml of 50% H_2O_2 and demineralized water until all sediment was immersed. Any remaining large organic fragments were removed with a 250 μm sieve. 10% HCl was then added to the sample (5 ml), and the sample was heated until boiling to dissolve the carbonate fraction. Water was added to until the samples were 800 ml in volume, left standing overnight, and decanted until ca. 100 ml the next day. A dispersant (300 mg $Na_4P_2O_2HCl_2O$) and 100 ml of demineralized water were added to the samples and heated until boiling, and when the samples reached room temperature, they were placed in the Laser Particle Sizer. Measurements were carried out after 3 min of ultrasonic treatment, and the analysis was performed using a Sympatec Helos (Helium–Neon Laser Optical System) Laser KR with Quixel dispersing system (range: 0.1–2000 μm, wet dispersion) at the Vrije Universiteit in Amsterdam.

Loss-on-ignition (LOI) was used to determine the bulk organic matter and calcium carbonate content of the sediment. Measurements were performed using a Leco TGA701, following preparation procedure of the sediment laboratory at the Vrije Universiteit Amsterdam. For each sample, 2 g of sediment was put in a plastic container and left overnight in the oven at 60 °C. The sediment was subsequently crushed to a fine powder, transferred to ceramic cups and placed in the Leco TGA701 furnace. During LOI measurements, the percentage of weight loss during each subsequent heating step was calculated, and translated into moisture (at 105 °C), total organic matter (at 550 °C), and carbonate content (at 1000 °C), respectively.

2.2.3. Charcoal analysis

A total of 122 sub-samples, each 0.5 cm^3 in volume, were collected every 2 cm from the entire core for macrocharcoal analysis. Subsamples were boiled in a 3% H_2O_2 solution for 60 min and then boiled in a 10% HCl solution for 60 min. The subsamples were subsequently washed on a 160 μm sieve, and charcoal particles were identified using a Zeiss microscope at 7–70x magnification. Image J was used to calculate the surface area of each charcoal fragment in a sample, and those measurements were converted to charcoal volume using the formula of Weng, (2005).

We processed 12 samples of 0.5 cm^3 each for pollen using standard laboratory techniques, and including *Lycopodium* tablets (Batch no: 483216, 18,583 spores per tablet) for calculating pollen concentration (Moore et al., 1991; Stockmarr, 1972). Pollen did not preserve in these samples, which is not unexpected given that Campo Libre is not a lake that would contain the anoxic conditions necessary for pollen preservation. We used these slides, however, to quantify the number of microscopic charcoal fragments found in these samples per number of *Lycopodium* encountered.

2.2.4. Phytolith analysis

Phytolith subsamples consisted of ca. 1 cm^3 of sediment collected at roughly 5 cm (between 3 and 10 cm) depth intervals throughout the core, for a total of 82 subsamples. Phytoliths were extracted from the sediments and samples were processed using standard laboratory procedures (Piperno, 2006). We added 56,000 microspheres to the subsamples before laboratory processing to calculate phytolith concentrations (Huisman et al., 2019).

Organic matter was removed from the phytolith samples using 3% H_2O_2 and $KMnO_4^-$. Carbonates were removed with 10% HCl. Phytoliths were extracted from the sediment by heavy liquid flotation using Bromoform at a specific gravity of 2.3, and mounted on microscope slides using Naphrax. Samples were analyzed with a Leica microscope using immersion oil and 630x magnification, and 250 phytoliths were identified per sample. Phytolith identification was based on literature (Morcote-Ríos et al., 2016; Morcote-Ríos et al., 2015; Piperno, 2006) and the phytolith reference collection of the University of Amsterdam.

2.3. Data analysis

Palm and grass genera are known to produce more than one type of phytolith (Morcote-Ríos et al., 2016; Morcote-Ríos et al., 2015; Piperno, 2006), thus we grouped palm phytolith morphotypes to known genus and grass phytolith morphotypes to known subfamily. These groupings were used to visually present the phytolith data and in the multivariate analyses. We also retained all morphotypes that could not be assigned to a genus or subfamily in the multivariate analyses. The phytolith assemblages were analyzed using constrained clustering analysis (CONISS) to identify major changes in vegetation composition through time (Grimm, 1987). We also analyzed the phytolith dataset with a detrended correspondence analysis (DCA) to assess the (dis)similarity of all samples (McCune and Grace, 2002).

2.4. Mapping the Campo Libre floodplain

We mapped the current landscape around the Campo Libre site using Shuttle Radar Topography Mission (SRTM) non-void filled elevation data at a spatial resolution of 1 arc-second (~30 m) (USGS, 2004). This dataset had missing elevation values (voids) that we filled with elevation data from the SRTM Void Filled dataset (Jarvis et al., 2008), which possessed a spatial resolution of 3 arc-seconds (~90 m). We delineated watershed boundaries in the Campo Libre region using the ArcHydro tools, following standard watershed modelling guidelines (Merwade, 2012). We calculated area of the Campo Libre watershed, and of the historic floodplain (fluvial terrace) where the Campo Libre core was collected. We also calculated statistics of forest cover (Hansen et al., 2013) for the bluff where Campo Libre was located. Three-dimensional images of the landscape were captured in ArcScene. All analyses were performed using ArcMap Version 10.6.

3. Results

3.1. Age-depth model

The 423-cm sediment core from Campo Libre spanned the last ca. 30,000 years (Table 1). Sedimentation was continuous, and there were no signs of reversals in dates (Table 1, Fig. 2). Sedimentation rates remained relatively continuous throughout the core, with an average sediment accumulation rate of 20 cm per 1000 years (50 years/cm) (Fig. 2). Sediment accumulation rates, however, slowed down at the level between 135 and 223 cm depth, which corresponded with ages of 17,000–13,000 cal yr BP (Table 1).

3.2. Particle size and loss-on-ignition analyses

Loss-on-ignition analysis indicated that the organic matter content of the Campo Libre core ranged from 8.5% to 40.4% and remained relatively stable throughout the entirety of the core (Fig. 3). Calcium carbonate values ranged from 0.7% to 2.7% in the core, with higher values prior to 18,000 cal yr BP than afterwards (Fig. 3). Particle size varied throughout the early sections of the core and became more stable after 17,000 cal yr BP (Fig. 3). Silty and clayey sediments dominated the majority of the core, but we identified two events with abrupt increases in sand deposition (Fig. 3). The earliest was recorded in several samples ranging from ca. 25,500 to 25,700 cal yr BP. The second occurred from ca. 17,600 to 18,500 cal yr BP.

3.3. Charcoal analysis

No macro-charcoal fragments were found in the 122 samples analyzed (Fig. 3). Of the 12 pollen slides scanned, only the samples with median ages of 357 and 3384 cal yr BP contained charcoal (Fig. 3). The remaining ten slides examined had ages ranging between 12,000 and 30,000 cal yr BP, and all of them lacked any evidence of microcharcoal (Fig. 3).

3.4. Phytolith analysis

A total of 60 phytolith types were observed in the samples, including 6 arboreal morphotypes, 11 palm morphotypes and 43 grass morphotypes (Table A1). The arboreal phytolith morphotypes could not be identified to family, but the palm morphotypes were identified to one or more genera, except in one case (Table A1). We named the unidentified palm morphotype *globular cavated stellate* (Fig. A1). Most of the globular echinate palm phytoliths originated from the genera *Euterpe* and *Geonoma* (Table A1). The conical palm phytoliths originated from genera such as *Bactris*, *Dictyocaryum*, *Wettinia*, *Chamaedorea*, *Aiphanes*, and *Geonoma* (Table A1). The grasses identified in the samples were all identified to at least subtribe (Table A1).

Phytolith influx rates ranged between ca. 125 x 10^3 and 18 x 10^6 phytoliths per cm^3 of sediment per year in the Campo Libre core (Fig. 3). The influx rates of grass morphotypes ranged between 113,344 and 15,904,000 phytoliths per cm^3 of sediment per year. Palm influx rates ranged between 0 and 10,752,000 phytoliths per cm^3 of sediment per year (Fig. 3). Arboreal influx rates ranged between 0 and 616,000 phytoliths per cm^3 sediment per year (Fig. 3). The highest peak in phytolith influx corresponded with peaks in the particle size and loss-on-ignition analyses (Fig. 3 and 360 cm depth).

Constrained clustering analysis (CONISS) indicated two major shifts in vegetation at Campo Libre over the last 30,000 years (Fig. 4). Zone CL1 (422–136 cm; 30,287–13,237 cal yr BP) was characterized by high percentages of grass phytoliths (81%–99%), low percentages of arboreal phytoliths (0%–8%), and low percentages of palm phytoliths (0%–16%). The Pharoideae and *Arundinella* grass morphotypes were more abundant in Zone CL1 compared with the other zones in the core (Fig. 4). The Pharoideae phytoliths decreased in abundance c. 18,500 cal yr BP, and the *Arundinella* morphotypes became very rare after the boundary between Zone CL1 and CL2.

Zone CL2 (136–80 cm, 13,237–7673 cal yr BP) was characterized by a sharp increase in palm phytoliths, with a peak c. 10,000 cal yr BP (Fig. 4). Total palm phytoliths ranged from 10% to 87% in Zone CL2, compared with 0%–16% in Zone CL1. The peak timings of the palms varied throughout Zone CL2 (Fig. 4). *Euterpe/Geonoma* phytoliths increased from 28% to a peak abundance of 49% between c. 12,200 and 10,000 cal yr BP. Conical Variant 3 palm phytoliths followed a similar pattern and peaked in abundance from 25% to 30% from c. 11,000 and 10,000 cal yr BP, compared with abundances of less than 17% in the rest of Zone CL2. Between c. 10,000 and 8300 cal yr BP, the globular cavated stellate palm phytoliths peaked in abundance (c. 4.6%) compared with elsewhere within the zone (<1.8%).

Arboreal phytoliths ranged from 0% to 6% in Zone CL2 (Fig. 4). Arboreal phytoliths decreased from 1 to 6% towards <1% between 11,600 and 9400 cal yr BP. From 8900 cal yr BP, arboreal phytoliths

Table 1
Radiocarbon dates and calibrated ages from the 423-cm sediment core collected from Campo Libre, Ecuador. Laboratory codes, core depth, sample weight, ^{14}C dates (±1 standard deviation), calibrated age ranges using IntCal13 and MatCal (Lougheed and Obrochta, 2016), and most likely age according to the Bacon age-depth model (Blaauw and Christen, 2011) (Fig. 2) are shown for each sample. All samples were calibrated using the IntCal13 calibration curve (Reimer et al., 2013). Numbers in parentheses indicate the probabilities of the samples falling within that age range. The sample with the asterisk (*) consisted of woody organic material, the other samples were bulk samples.

Laboratory Code	Core depth (cm)	Weight (g)	^{14}C yr BP ± 1 SD	Intcal13 Calibrated age range (2σ)	Bacon age-depth model age-range (2σ)	Bacon age-depth model weighted mean age (cal yr BP)
Ua-53644	32	0.034*	2492 ± 29	2725-2465 (0.955)	2733.8-1441.8	2459.2
CL1_43_44	43	1.5	1889 ± 26	3141-3118 (0.032) 3113-3093 (0.03) 3079-2945 (0.89) 2931-2930 (0.002)	3689.9-1796.6	2891.6
CL2_104_105	104	1	8733 ± 55	9905-9550 (0.955)	10,131.2-9424.6	9737.1
CL2_135_135	135	1.4	11,298 ± 43	13,252-13,070 (0.955)	13,348.7-12,927.1	13,188.9
CL3-63-64_278-279	223	1.1	13,766 ± 62	16,917-16,372 (0.955)	17,380.9-16,454	16,842.2
CL4_85-86-370-371	311	1	20,643 ± 89	25,204-24,511 (0.955)	25,257.6-24,122.3	24,756
CL5_10–11_390-391	334	1.4	21,733 ± 100	26,161-25,790 (0.955)	26,392.7-25,710.8	26,046.6
Ua-53645	401.5	5	25,405 ± 118	29,853-29,099 (0.955)	30,132.5-28,973.8	29,547.3

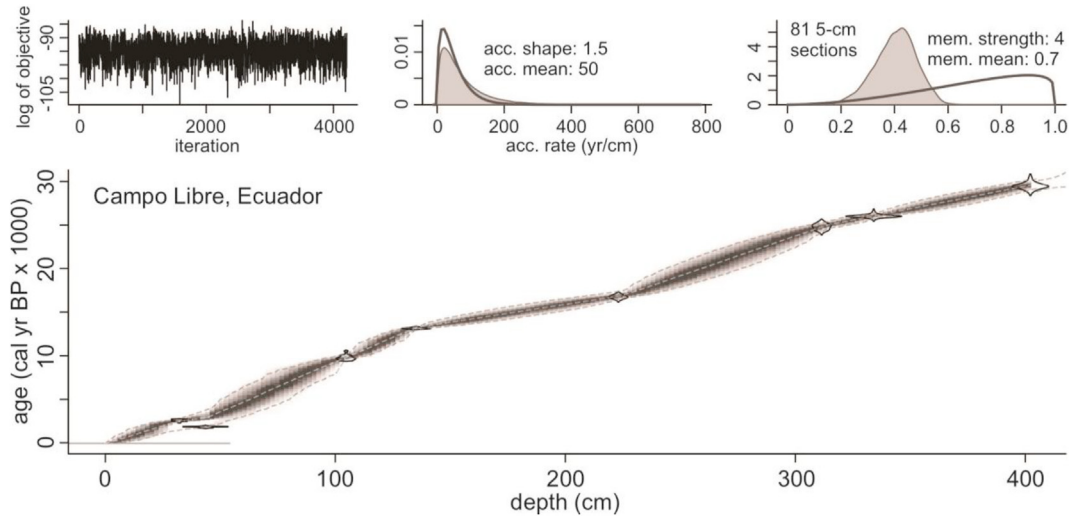

Fig. 2. Bacon age-depth model for the 423-cm sediment core obtained from Campo Libre, Ecuador. The ^{14}C AMS dates obtained on the core (Table 1) are shown as polygons. Darker shading represents the most likely ages of the samples. The white dashed line represents the mean value of likely ages, and the black dashed lines represent the 95% confidence intervals. Sediment accumulation rates (years per centimeter) and memory, a metric of temporal autocorrelation scaled from 0 (none) to 1 (linear), are shown.

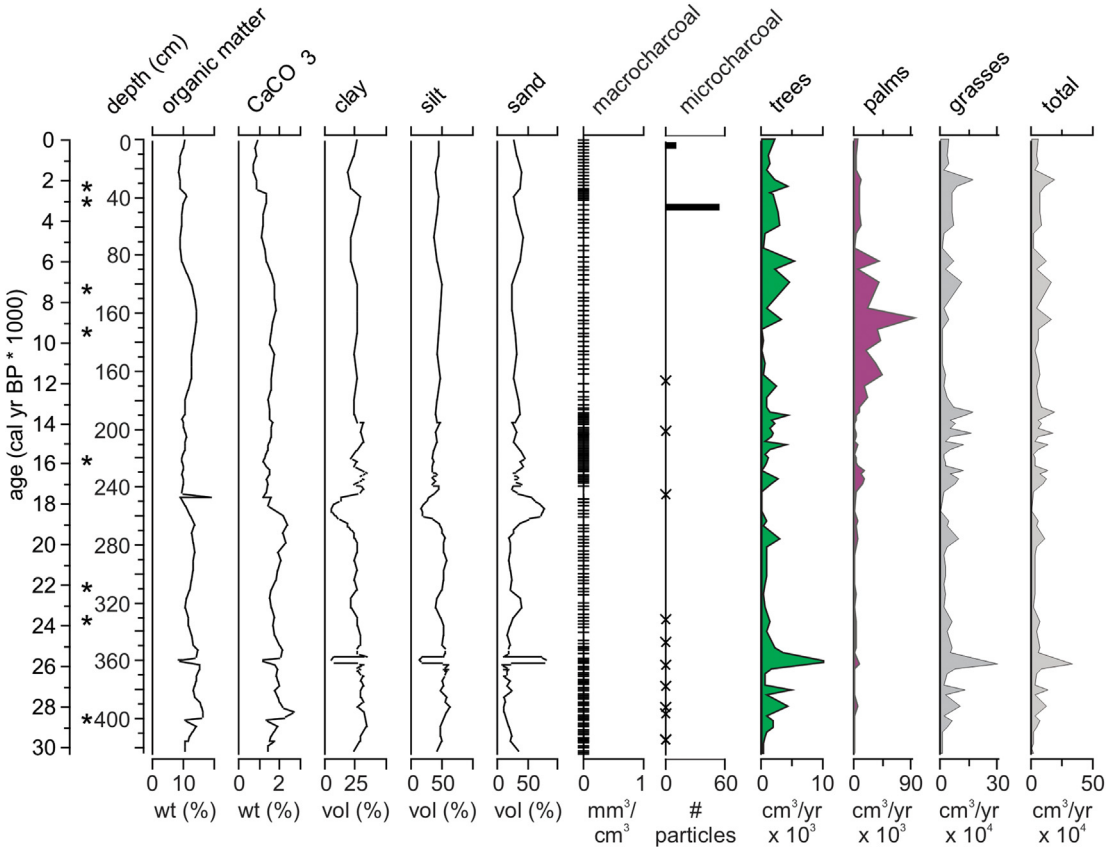

Fig. 3. Loss-on-ignition, particle size, charcoal, and phytolith results for Campo Libre, Ecuador. The first two columns indicate the age-depth relationship, and the asterisks (*) indicate the depth of ^{14}C AMS dated material (Table 1, Fig. 2). Percentages of organic matter, calcium carbonate ($CaCO_3$), clay, silt, and sand are shown. Macroscopic and microscopic charcoal results are shown. The absence of charcoal is indicated with + and x, respectively, for the macroscopic and microscopic measurements. Arboreal (tree), palm, grass, and total phytolith influx rates are also shown.

increased with an occurrence around 2% at the top of the zone. Grass phytolith percentages within Zone CL2 ranged from 12% to 89%, with a significant amount of variation within the zone (Fig. 4). Grass phytoliths declined rapidly from 88% at the bottom of the zone to 12% at c. 10,000 cal yr BP, after which they increased again up to 42% (Fig. 4).

Zone CL3 (80–0 cm, 7673 cal yr BP - modern) was characterized by a high percentage of grasses from ca. 7600 - 5300 cal yr BP (61%–

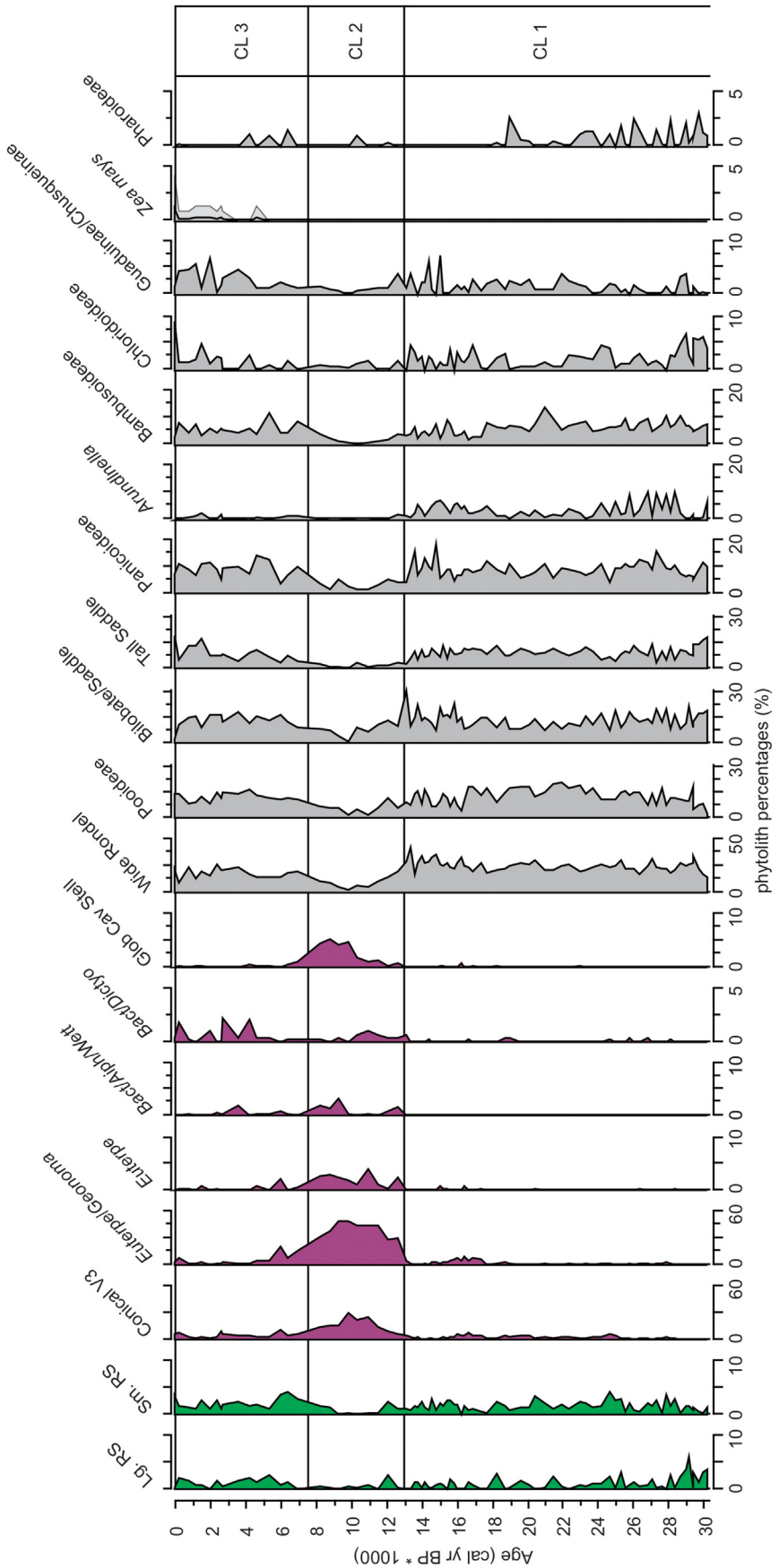

Fig. 4. Stratigraphic diagram of the most common phytolith morphotypes found in the Campo Libre (Ecuador) sediment core. Arboreal morphotypes are shown in green, palm morphotypes are shown in purple, and grass morphotypes are shown in grey. *Zea mays* is shown with 3x exaggeration in light grey. (For interpretation of the references to color in this figure legend, the reader is referred to the Web version of this article.)

90%). Narrow elliptical phytoliths increased in abundances from 4212 cal yr BP (up to 7%). Palm phytoliths ranged between 5% and 35% of the assemblages, but decreased in abundance gradually from the bottom towards the top of this zone (Fig. 4). Conical variant 1 phytoliths, which are produced by *Bactris, Aiphanes*, and *Wettinia*, increased from <1% to >2% from 4213 cal yr BP until the present. Arboreal phytoliths ranged between 1% and 5% throughout Zone CL3. Maize phytoliths first appeared at 4663 cal yr BP, and occurred regularly between 0.3 and 1.1% from ca. 2800 cal yr BP until the present (Fig. 4).

The detrended correspondence analysis (DCA) indicated that Zones CL1 and CL3 were similar in composition, and both dominated by grass taxa (Figs. 4 and 5). The first axis of the DCA explained 28.9% of the variance in the dataset, and separated the sites containing high abundances of palm taxa (Zone CL2) from those that had low palm abundances (Zones CL1 and CL3) (Fig. 5). These results agreed with the zonation of the CONISS analysis. The second DCA axis explained 4.6% of the variance, and separated palm types, grass types, and forest types (Fig. 5). The conical variant 3 palm phytoliths were ca. 2 standard deviations (units of DCA axes) away on the positive end of DCA Axis 2 compared with the other palm phytolith morphotypes. Samples with higher abundances of the *Arundinella* phytoliths were on the negative side of DCA Axis 2, whereas samples with higher abundances of Phariodeae and Chloridoideae grasses, and samples containing maize phytoliths, were located on the positive end. The large rugose spheres occurred primarily alongside Chloridoideae and Pharoideae grasses and conical variant 3 palm phytoliths. The small rugose spheres were found in samples with higher abundances of Panicoideae and Bambusoideae grasses (Fig. 5).

3.5. Mapping Campo Libre

Campo Libre lies in a watershed that includes 1529 km^2 in area, and the core site was located on a relatively flat fluvial terrace that is ca. 7.28 km^2 in area (Fig. 6). The mean forest cover from A.D. 2000 to 2012 on the Campo Libre floodplain was 45.9%, with a standard deviation of 34.0%. The terrace was surrounded by forested mountains exceeding 2500 m above sea level, except where it was bounded by the river (Fig. 6). The adjacent watershed also included a historic floodplain or fluvial terrace setting similar to Campo Libre.

4. Discussion

4.1. Landscape and vegetation dynamics at Campo Libre

The Quijos River dynamics currently do not affect the Campo Libre site (Fig. 6c). This was not the case in the past, as tectonic activity and river dynamics have formed the modern fluvial terrace formation (de Berc et al., 2005). Modern incision rates measured on the Pastaza River near the Mera formation (Fig. 1) are estimated to be 0.5 cm/year (de Berc et al., 2005). This has likely varied through time, but if it were used as an average incision rate, the elevation difference between the current alluvial terrace and the Quijos River (ca. 9000 cm) would suggest that the historic floodplain became inactive ca. 18,000 cal yr BP. The period between 18,000 and 17,000 cal yr BP was the last time in the Campo Libre record where the sediment analysis registered a likely flood event, i.e. a peak in sand percentages and decreases in silt and clay percentages (Fig. 3). Though the driver of this flood event remains unknown, the stabilization of the particle sizes and sediment properties (Fig. 3), and several trends noted in the phytolith record, suggest the terrace became shut off from constant river input c. 18,000–17,000 cal yr BP (Fig. 4).

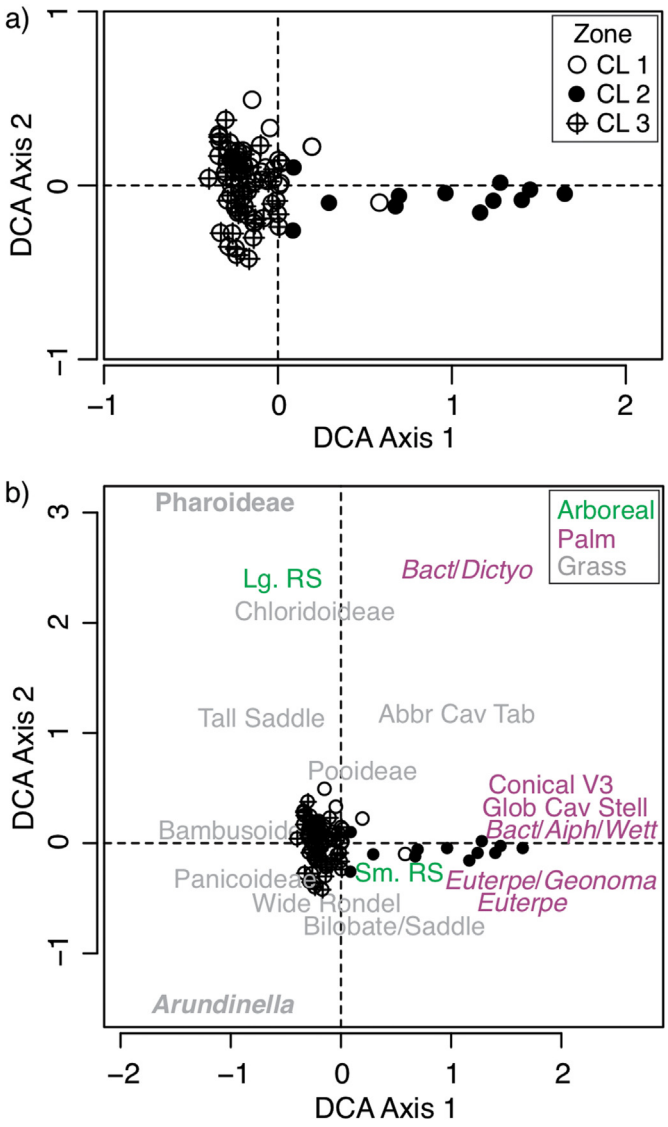

Fig. 5. Detrended correspondence analysis of phytoliths found in the sediment core from Campo Libre, Ecuador. a) Site (sample scores) shown for Zones CL1-CL3 as shown in Fig. 4 b) Site-species scores for the phytolith types found in the Campo Libre core. Phytolith morphotypes are color-coded into arboreal (tree), palm, and grass groups as shown in Fig. 4. (For interpretation of the references to color in this figure legend, the reader is referred to the Web version of this article.)

Prior to 18,000–17,000 cal yr BP, besides local deposition, phytoliths were also being transported and deposited by the river, and originating from upslope within the watershed (Fig. 6b and c). Campo Libre contained lower concentrations of phytoliths prior to 18,000 cal yr BP compared with afterwards, and palm concentrations are particularly low (Figs. 3 and 4). When Campo Libre was an active part of the river system, grasses of the Pharoideae subtribe were present and composed up to 3% of the total phytolith assemblage (Fig. 4). After the floodplain became inactive, these grasses completely disappear in Zone CL1, and only sporadically return later in the record (Fig. 4). Pharoideae grasses evolved in closed forest environments, and currently inhabit shaded tropical forests (Bouchenak-Khelladi et al., 2010). It is thus likely that the Pharoideae grasses in the Campo Libre phytolith percentages are derived primarily from forested local or regional sources, via the river or from the downwash of phytoliths from the surrounding hillsides (Fig. 7a). After 18,000–17,000 cal yr BP, the phytolith

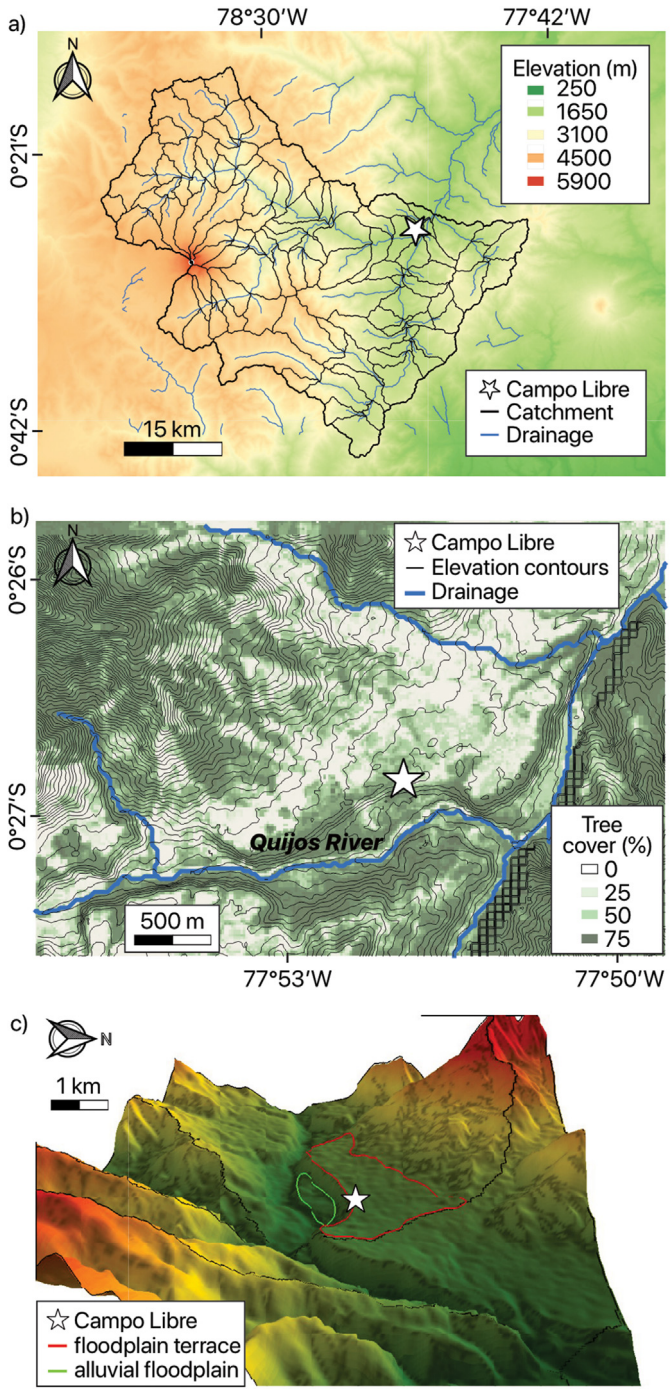

Fig. 6. Topographical and hydrological information on the Campo Libre core site and surrounding areas. a) The catchment boundaries (black lines) and drainage systems (blue lines) for Campo Libre (star) are shown alongside elevation. b) Campo Libre (star) lies on the modern floodplain, which is the area surrounded by drainages (blue lines), including the Quijos River to the south. Forest cover data from 2010 (Hansen et al., 2013) around the catchments is shown. c) Three-dimensional ArcScene view of the bluff where the Campo Libre core (star) was retrieved, the Quijos River valley, and the surrounding hills. (For interpretation of the references to color in this figure legend, the reader is referred to the Web version of this article.)

source area becomes primarily localized to the Campo Libre fluvial terrace (Fig. 7b), with a small potential input from the downwash of the surrounding slopes.

Palm phytolith concentrations and percentages were low during the glacial period at Campo Libre. Palms produce an abundance of phytoliths (Piperno, 2006; Piperno et al., 2019), and if they were growing in the local vicinity, it is likely that they would be seen in our samples. Palms are present but in low abundances at the Mera and San Juan Bosco sites from 33,000–26,000 cal yr BP (Bush et al., 1990; Loughlin et al., 2018a) (Fig. 1a). These sites lie between 900 and 1100 m above sea level (masl), and are located c. 120 km to the south of Campo Libre, which lies at 1800 masl (Fig. 1). Lake Pindo, located at 1300 masl near Mera, and Lake Consuelo, located at 1300 masl in southern Peru, also contain low amounts of palms in the last glacial period (Montoya et al., 2018; Urrego et al., 2010). Palms are common features of the modern mid-elevation Andean forests (Svenning et al., 2009), but collectively, these data suggest that palms occurred in much lower abundances in these forests during the last glacial period.

The biggest changes in vegetation documented in the Campo Libre record began ca. 12,900 cal yr BP (Fig. 4), corresponding with the transition between the Antarctic Cold Reversal (ACR, also called Bølling-Alleröd in the Northern Hemisphere) and the Younger Dryas (YD) period (Fig. 8) (Jomelli et al., 2014). Palm concentrations and percentages significantly increase during the ACR-YD transition, but the major changes in arboreal taxa instead begin at the Pleistocene-Holocene transition (Fig. 8). During the Holocene, palm abundances at Campo Libre closely track changes in precipitation inferred from nearby stalagmite records (Bustamante et al., 2016; Mosblech et al., 2012; van Breukelen et al., 2008) (Fig. 8). These data suggest that precipitation change during the Holocene has been one of the most important drivers of palm distributions and abundances in mid-elevation Andean forests. Insolation, or solar forcing, and changes in Equatorial Pacific sea-surface temperatures are believed to have driven these precipitation changes (Mosblech et al., 2012; Seillès et al., 2016; van Breukelen et al., 2008).

At the onset of CL2, when temperatures were still cool and precipitation started to decrease (Fig. 8), *Euterpe* and *Geonoma* species started to grow around Campo Libre (Fig. 4). *Euterpe precatoria* is one of the commonest species in the Amazon lowlands (ter Steege et al., 2013), and is the only *Euterpe* species that ascends to 2000 masl on the Andean slopes (Moraes et al., 1995). *Euterpe precatoria* also prefers to be topographically higher and drier, and not located in swampy conditions (Svenning, 1999). Between 10,000 and 9000 cal yr BP, global temperatures continued to rise (e.g. Masson-Delmotte et al., 2005; Rasmussen et al., 2014), but regional precipitation began to increase (Mosblech et al., 2012), and palm genera such as *Chamaeodorea, Wettinia, Aiphanes* or *Bactris* and an unknown palm began to replace *Euterpe* and *Geonoma* (Fig. 4). These genera are all currently found in mid-elevation Andean forests (Svenning, 2001a, 2001b; Svenning et al., 2009).

Arboreal and grass phytoliths also responded to Holocene precipitation change, decreasing in abundance from 11,800 cal yr BP to ca. 9000 cal yr BP, a period of decreased regional precipitation (Fig. 8), and the transition of the system from a swamp to a palm forest (Fig. 7c). The percentages of arboreal and grass phytoliths increase towards the end of Zone CL2, again coincident with regional records of increased precipitation (Fig. 8). The boundary between Zones CL2 and CL3 likely represents the point at which precipitation became sufficiently more abundant to transition the system from a palm forest back into a grassy swamp (Fig. 7c and d).

Arundinella species, such as *A. hispida*, grow in South America in wet grounds, seasonally inundated savannas, and montane forest edges up to 2000 masl (Quattrocchi, 2006; Veldkamp, 2015). Thus, *Arundinella* may indicate wetter conditions as it disappears during the drier period of CL2 (Fig. 4). When precipitation increases after 7500 cal yr BP (Fig. 8), it reappears but its occurrence is not as abundant as when Campo Libre was an active floodplain (Fig. 7d). Campo Libre remained a grassy swamp until the onset of local human occupation, ca. 4300 cal yr BP (Figs. 4 and 7). The Campo

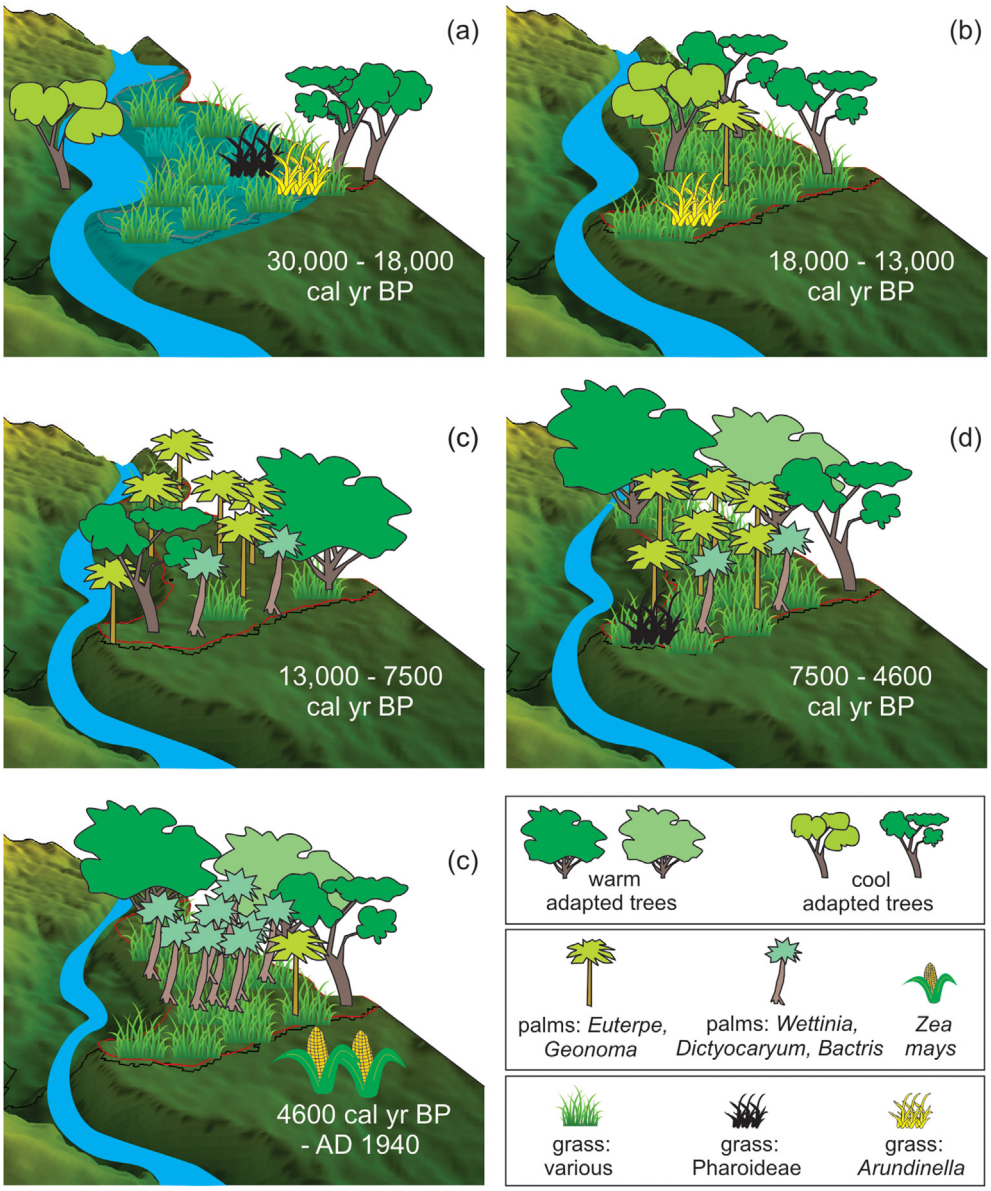

Fig. 7. Landscape and vegetation reconstructions through time. The background landscape is from the 3D ArcScene image (Fig. 6c), and vegetation and river dynamics are based on data presented in Figs. 3 and 4. Panels a–e show the general change of the system through time.

Libre phytolith record did not have sufficient temporal resolution to assess vegetation response to regional precipitation variability that has occurred over the last c. 2000 years (Ledru et al., 2013), leaving the relative effect of climate versus anthropogenic forcing during this period unknown.

4.2. Human occupation at Campo Libre

The first sign of localized human occupation at Campo Libre occurred in the form of maize phytoliths found at ca. 4700 cal yr BP (Fig. 4), after the site had transitioned from a palm forest to a grassy swamp (Fig. 7d). Regional burning (via microscopic charcoal) was documented at ca. 3400 cal yr BP, and by ca. 2800 cal yr BP, maize occurred regularly in the record until the present day (Figs. 3–4, 7e). After 5000 cal yr BP, percentages of *Bactris* phytoliths also increase to levels higher than seen at any other point in the history of the site, suggesting that palm cultivation may have accompanied maize cultivation at Campo Libre. Guaduinae and Chusqueinae grasses (bamboos) increased after the onset of maize cultivation (Fig. 4). Bamboos are common elements in forest openings and disturbances in tropical forests, and the increases in bamboo species may alter long-term dynamics among arboreal species (Fadrique et al., 2021; Griscom and Ashton, 2006; Larpkern et al., 2011).

Our findings agree with previous paleoecological reconstructions from the Huila core collected ca. 15 km upriver of Baeza (Fig. 1). Maize cultivation was present at Huila from the base of the core at 700 cal yr BP until European arrival to the Americas (Loughlin et al., 2018b). The Huila core contained evidence of large-scale burning around ca. 350 cal yr BP, which is when we found evidence of regional burning (i.e. microcharcoal) at Campo Libre (Fig. 3). It is also possible that maize cultivation at Huila occurred for the same duration as at Campo Libre, as the sites are so close in proximity (Fig. 1). It is interesting, however, that maize cultivation

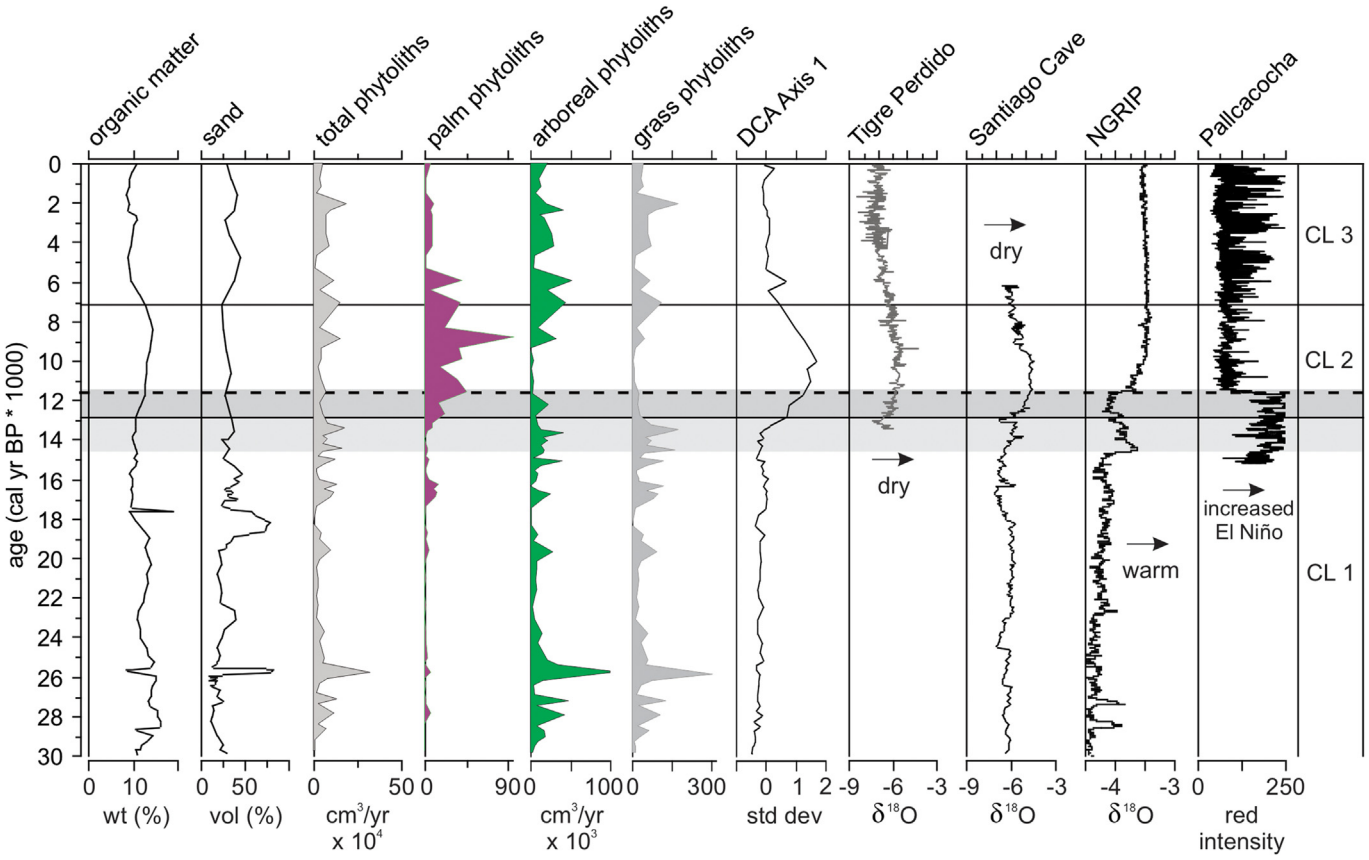

Fig. 8. Summary figure of local proxies of environmental change from Campo Libre compared with regional and global paleoclimate reconstructions. Organic matter percentage, sand percentage, phytolith concentrations, and DCA Axis 1 from Campo Libre are shown in comparison with global and regional climate records. The $\delta^{18}O$ records from the Tigre Perdido (van Breukelen et al., 2008) and Santiago Cave (Mosblech et al., 2012) stalagmites (Fig. 1) represent local and regional precipitation. The $\delta^{18}O$ record from the NGRIP ice core record represents northern hemisphere temperature change (Rasmussen et al., 2014). Red intensity values from Laguna Pallcacocha (Fig. 1) represent regional El Niño frequency (Moy et al., 2002). The solid horizontal lines show the major changes in vegetation indicated by CONISS analysis, and the dashed horizontal line represents the Pleistocene-Holocene boundary. Light grey shading represents the Antarctic Cold Reversal (or Bølling-Alleröd in the Northern Hemisphere), and dark grey shading represents the Younger Dryas.

continues through the post-Colonial period at Campo Libre (Figs. 4 and 8), whereas it ceases at Huila (Loughlin et al., 2018b).

The onset of maize cultivation at Campo Libre fell within periods of known occupation and cultivation in the neighboring lowlands and highlands. Lake Ayauch[i] is 300 km south of Campo Libre and downslope in the Amazonian lowlands (Fig. 1). Maize cultivation at Lake Ayauch[i] began as early as 6000 cal yr BP, and increased in frequency ca. 2500 cal yr BP (Bush et al., 1989). Lake Sauce, located further south in Peru and also in the Amazonian lowlands, shows a similar timing in the onset and increase in maize frequency (Bush et al., 2016). Maize cultivation has been found in the Andean highlands of Colombia as early as 8000 years ago, and on the coasts of Ecuador c. 7000 years ago (Pearsall, 2008). Campo Libre lies in one of the most important valleys connecting the Andean highlands and Amazonian lowlands (Fig. 1), making it a very likely place to find the earliest onset of maize cultivation in the mid-elevation forests. Our data suggest that maize cultivation began c. 1000–1500 years later in the mid-elevation forests compared with the upslope and downslope regions.

5. Conclusion

Paleoecological archives in the mid-elevation forests of the Andes are a rarity, and very few existing records span the last glacial-interglacial transition and onset of humans in the landscape (Bush et al., 1990; Cárdenas et al., 2014; Montoya et al., 2018; Urrego et al., 2010). Part of the rarity of archives is because most paleoecological reconstructions rely on pollen grains, which oxidize and do not preserve in many conditions. Phytoliths preserve in places where pollen grains do not, such as Campo Libre, but so far have only been analyzed in one study containing sediments from the last glacial period (Bush et al., 1990). Our phytolith record demonstrates the sensitivity and usefulness of phytoliths in detecting landscape changes, changes in vegetation composition, and human influences on vegetation communities in mid-elevation Andean forests (Figs. 4–5, 7).

We have reconstructed 30,000 years of landscape and vegetation dynamics at Campo Libre, located at 1800 masl in the Ecuadorian Andes. We estimate that Campo Libre was a part of the Quijos River floodplain until ca. 18,000 years ago, based on known incision rates in the region, and our sedimentary and phytolith analyses. The largest vegetation changes documented at Campo Libre do not occur when the floodplain became inactive, but instead occur at the Pleistocene-Holocene transition and as a result of insolation-driven precipitation changes in the Holocene. Local human influence and regional fire activity appeared in the late Holocene, and continued to the present. There was no sign of population collapse or the end of maize cultivation when Europeans arrived in the region.

Data availability

All data from this manuscript will be uploaded into the NEOTOMA paleoecological database (neotomadb.org) and Data Dryad (datadryad.org) upon publication.

Declaration of competing interest

The authors declare that they have no known competing financial interests or personal relationships that could have appeared to influence the work reported in this paper.

Acknowledgements

We would like to thank Joe Williams and Macarena Cardenas for their assistance with fieldwork, Isa Mulder for assisting with the charcoal analysis, and Annemarie Phillip for the processing of phytolith and pollen samples. This work is a part of a NASA Interdisciplinary Research in Earth Science NNX14AD31G to C.N.H.M., and was also supported by funds from the Open University to W.D.G. We would also like to thank the Royal Botanic Garden Edinburgh, Santander, and the British Ecological Society (small ecological project grant #1052/1947) for supporting the project. This work was also supported by the MSc Biology and MSc Earth Sciences programs in the Institute for Biodiversity and Ecosystem Dynamics at the University of Amsterdam. B.C.L. and the ^{14}C dates obtained from Uppsala were funded by Swedish Research Council (Vetenskapsrådet) grant number 637-2014-499.

Appendix A. Supplementary data

Supplementary data to this article can be found online at https://doi.org/10.1016/j.quascirev.2021.106866.

References

Åkesson, C.M., Matthews-Bird, F., Bitting, M., Fennell, C.-J., Church, W.B., Peterson, L.C., Valencia, B.G., 2019. 2,100 years of human adaptation to climate change in the High Andes. Nat. Ecol. (Evolution), 1–9.
Athens, J.S., Ward, J.V., Pearsall, D.M., Chandler-Ezell, K., Blinn, D.W., Morrison, A.E., 2016. Early Prehistoric maize in northern highland Ecuador. Lat. Am. Antiq. 27, 3–21.
Blaauw, M., Christen, J.A., 2011. Flexible paleoclimate age-depth models using an autoregressive gamma process. Bayesian Analysis 6, 457–474.
Bouchenak-Khelladi, Y., Verboom, G.A., Savolainen, V., Hodkinson, T.R., 2010. Biogeography of the grasses (Poaceae): a phylogenetic approach to reveal evolutionary history in geographical space and geological time. Bot. J. Linn. Soc. 162, 543–557.
Bush, M., Correa-Metrio, A., Mcmichael, C., et al., 2016. A 6900-year history of landscape modification by humans in lowland Amazonia. Quat. Sci. Rev. 141, 52–64.
Bush, M.B., Alfonso-Reynolds, A.M., Urrego, D.H., Valencia, B.G., Correa-Metrio, Y.A., Zimmermann, M., 2015. Fire and climate: contrasting pressures on tropical Andean timberline species. J. Biogeogr. 42, 938–950.
Bush, M.B., Colinvaux, P.A., Wiemann, M.C., Piperno, D.R., Liu, K.-B., 1990. Late Pleistocene temperature depression and vegetation change in Ecuadorian Amazonia. Quat. Res. 34, 330–345.
Bush, M.B., Flenley, J., Gosling, W.D., 2011. Tropical Rainforest Responses to Climatic Change. Springer Science & Business Media.
Bush, M.B., Gosling, W.D., 2012. Environmental change in the humid tropics and monsoonal regions. In: Matthews, J.A., Al, E. (Eds.), The SAGE Handbook of Environmental Change: Volume 2. Human Impacts and Response. Sage, London.
Bush, M.B., Mcmichael, C.H., Raczka, M.F., De Toledo, M.B., Power, M.J., Mayle, F.E., De Oliveira, P.E., 2014. The Holocene of the Amazon. In: Carvalho, I.S., Garcia, M.J., Lana, C.C., Strohschoen Jr., O. (Eds.), Paleoclimas - Série Paleontologia: Cenários de Vida. Page. Sao Paulo, Brazil, Interciência.
Bush, M.B., Piperno, D.R., Colinvaux, P.A., 1989. A 6000 year history of Amazonian maize cultivation. Nature 340, 303–305.
Bustamante, M.G., Cruz, F.W., Vuille, M., et al., 2016. Holocene changes in monsoon precipitation in the Andes of NE Peru based on δ18O speleothem records. Quat. Sci. Rev. 146, 274–287.
Cárdenas, M.L., Gosling, W.D., Pennington, R.T., Poole, I., Sherlock, S.C., 2014. Forests of the tropical eastern Andean flank during the middle Pleistocene. Palaeogeogr. Palaeoclimatol. Palaeoecol. 393, 76–89.
Clark, P.U., Shakun, J.D., Baker, P.A., et al., 2012. Global climate evolution during the last deglaciation. Proc. Natl. Acad. Sci. Unit. States Am. 109, E1134–E1142.
Colinvaux, P.A., De Oliveira, P.E., Moreno, J.E., Miller, M.C., 1996. A long pollen record from lowland Amazonia: Forest and cooling in glacial times. Science 274, 85–88.
Colwell, R.K., 2000. The mid-domain effect: geometric constraints on the geography of species richness. Trends Ecol. Evol. 15, 70–76.
Conroy, J.L., Overpeck, J.T., Cole, J.E., 2010. El Niño/Southern Oscillation and changes in the zonal gradient of tropical Pacific sea surface temperature over the last 1.2 ka, 18, 32–34.
Cuesta, F., Llambí, L.D., Huggel, C., et al., 2019. New land in the Neotropics: a review of biotic community, ecosystem, and landscape transformations in the face of climate and glacier change. Reg. Environ. Change 1–20.
De Berc, S.B., Soula, J., Baby, P., Souris, M., Christophoul, F., Rosero, J., 2005. Geomorphic evidence of active deformation and uplift in a modern continental wedge-top–foredeep transition: example of the eastern Ecuadorian Andes. Tectonophysics 399, 351–380.
Fadrique, B., Santos-Andrade, P., Farfan-Rios, W., Salinas, N., Silman, M., Feeley, K.J., 2021. Reduced tree density and basal area in Andean forests are associated with bamboo dominance. For. Ecol. Manag. 480, 118648.
Flantua, S., Hooghiemstra, H., Vuille, M., et al., 2016. Climate variability and human impact in South America during the last 2000 years: synthesis and perspectives from pollen records. Clim. Past 12, 483–523.
Goldberg, A., Mychajliw, A.M., Hadly, E.A., 2016. Post-invasion demography of prehistoric humans in South America. Nature 532, 232–235.
Grimm, E.C., 1987. CONISS: a fortran 77 program for stratigraphically constrained cluster analysis by the method of incremental sum of squares. Comput. Geosci. 13, 13–35.
Griscom, B., Ashton, P., 2006. A self-perpetuating bamboo disturbance cycle in a neotropical forest. J. Trop. Ecol. 22, 587–597.
Groot, M.H.M., Bogotá, R.G., Lourens, L.J., et al., 2011. Ultra-high resolution pollen record from the northern Andes reveals rapid shifts in montane climates within the last two glacial cycle. Clim. Past 7, 299–316.
Hagemans, K., Tóth, C.-D., Ormaza, M., Gosling, W.D., Urrego, D.H., León-Yánez, S., Wagner-Cremer, F., 2019. Modern pollen-vegetation relationships along a steep temperature gradient in the Tropical Andes of Ecuador. Quat. Res. 92, 1–13.
Hansen, M., Potapov, P., Moore, R., et al., 2013. High-resolution global maps of 21st-century forest cover change. Science 15, 850–853.
Hooghiemstra, H., Cleef, A., 1995. Pleistocene climatic change and environmental and generic dynamics in the north Andean montane forest and paramo. In: Churchill, S.P., Balsev, H., Forero, E. (Eds.), Biodiversity and Conservation of Neotropical Montane Forests. The New York Botanical Garden, New York.
Huisman, S.N., Bush, M.B., Mcmichael, C.N., 2019. Four centuries of vegetation change in the mid-elevation Andean forests of Ecuador. Veg. Hist. Archaeobotany 28, 679–689.
Huisman, S.N., Raczka, M.F., 2018. Palm Phytoliths of Mid-Elevation Andean Forests. Front. Ecol. Evol. 6, 193.
Jarvis, A., Reuter, H.I., Nelson, A., Guevara, E., 2008. Hole-filled SRTM for the Globe Version 4. Available from the CGIAR-CSI SRTM 90m Database http://srtm. csi. cgiar. org.
Jomelli, V., Favier, V., Vuille, M., et al., 2014. A major advance of tropical Andean glaciers during the Antarctic cold reversal. Nature 513, 224–228.
Jørgensen, P.M., Ulloa Ulloa, C., León, B., León-Yánez, S., Beck, S.G., Nee, M., Zarucchi, J.L., Celis, M., Bernal, R., Gradstein, R., 2011. Regional patterns of vascular plant diversity and endemism. In: Climate Change and Biodiversity in the Tropical Andes. Inter-American Institute for Global Change Research (IAI) and Scientific Committee on Problems of the Environment (SCOPE), pp. 192–203.
Larpkern, P., Moe, S.R., Totland, Ø., 2011. Bamboo dominance reduces tree regeneration in a disturbed tropical forest. Oecologia 165, 161–168.
Ledru, M.-P., Jomelli, V., Samaniego, P., Vuille, M., Hidalgo, S., Herrera, M., Ceron, C., 2013. The medieval climate anomaly and the little ice age in the eastern Ecuadorian Andes. Clim. Past 9, 307–321.
Liu, K., Colinvaux, P.A., 1985. Forest changes in the Amazon Basin during the last glacial maximum. Nature 318, 556–557.
Lougheed, B., Obrochta, S., 2016. MatCal: open source bayesian 14 C age calibration in MatLab. J. Open Res. Software 4.
Loughlin, N.J., Gosling, W.D., Coe, A.L., Gulliver, P., Mothes, P., Montoya, E., 2018a. Landscape-scale drivers of glacial ecosystem change in the montane forests of the eastern Andean flank, Ecuador. Palaeogeogr. Palaeoclimatol. Palaeoecol. 489, 198–208.
Loughlin, N.J., Gosling, W.D., Mothes, P., Montoya, E., 2018b. Ecological consequences of post-Columbian indigenous depopulation in the Andean–Amazonian corridor. Nature Ecology & Evolution 2, 1233–1236.
Masson-Delmotte, V., Landais, A., Stievenard, M., et al., 2005. Holocene climatic changes in Greenland: different deuterium excess signals at Greenland ice core project (GRIP) and NorthGRIP. J. Geophys. Res.: Atmosphere 110.
Matthews-Bird, F., Valencia, B.G., Church, W., Peterson, L.C., 2017. A 2000-year history of disturbance and recovery at a sacred site in Peru's northeastern cloud forest. The Holocene, 0959683617702232.
Mayle, F.E., Power, M.J., 2008. Impact of a drier early–mid-holocene climate upon amazonian forests. Phil. Trans. Biol. Sci. 363, 1829–1838.
McCune, B., Grace, J.B., Gleneden Beach, Oregon, 2002. Analysis of Ecological Communities. MJM Software Design.
McMichael, C., Piperno, D.R., Bush, M.B., Silman, M.R., Zimmerman, A.R.,

Raczka, M.F., Lobato, L.C., 2012. Sparse pre-Columbian human habitation in western Amazonia. Science 336, 1429–1431.
Merwade, V., 2012. Watershed and Stream Network Delineation Using ArcHydro Tools. University of Purdue, School of Civil Engineering, Printed Lecture Note, USA.
Montoya, E., Keen, H.F., Luzuriaga, C.X., Gosling, W.D., 2018. Long-term vegetation dynamics in a megadiverse hotspot: the ice-age record of a pre-montane forest of central Ecuador. Front. Plant Sci. 9, 196.
Moore, P.D., Webb, J.A., Collinson, M.E., 1991. Pollen Analysis. Blackwell Scientific, Oxford.
Moraes, M., Galeano, G., Bernal, R., Balslev, H., Henderson, A., 1995. Tropical andean palms (arecaceae). In: Churchill, S.P., Balslev, H., Forero, E., Luteyn, J.L. (Eds.), Biodiversity and Conservation of Neotropical Montane Forest. Page. New York, New York Botanical Garden.
Morcote-Ríos, G., Bernal, R., 2016. Phytoliths as a tool for archaeobotanical, palaeobotanical and palaeoecological studies in Amazonian palms. Bot. J. Linnean Soc. 182, 348–360.
Mosblech, N.A., Bush, M.B., Gosling, W.D., et al., 2012. North Atlantic forcing of Amazonian precipitation during the last ice age. Nat. Geosci. 5, 817–820.
Moy, C.M., Seltzer, G.O., Rodbell, D.T., Anderson, D.M., 2002. Variability of El nino/southern oscillation activity at millennial timescales during the Holocene epoch. Nature 420, 162–164.
Myers, N., Mittermeier, R.A., Mittermeier, C.G., Da Fonseca, GaB., Kent, J., 2000. Biodiversity hotspots for conservation priorities. Nature 403, 853–858.
Pearsall, D.M., 2008. Plant domestication and the shift to agriculture in the Andes. In: Silverman, H., Isbell, W.H. (Eds.), The Handbook of South American Archaeology. New York, Springer, New York.
Piperno, D.R., 2006. Phytoliths: A Comprehensive Guide for Archaeologists and Paleoecologists. Alta Mira Press, Lanham, MD.
Piperno, D.R., Mcmichael, C.N., Bush, M.B., 2019. Finding forest management in prehistoric Amazonia. Anthropocene 26, 100211.
Quattrocchi, U., 2006. CRC World Dictionary of Grasses: Common Names, Scientific Names, Eponyms, Synonyms, and Etymology-3 Volume Set. CRC Press.
R Development Core Team, 2013. R: A Language and Environment for Statistical Computing. R Foundation for Statistical Computing, Vienna, Austria.
Rademaker, K., Hodgins, G., Moore, K., et al., 2014. Paleoindian settlement of the high-altitude Peruvian Andes. Science 346, 466–469.
Rahbek, C., 1995. The elevational gradient of species richness: a uniform pattern? Ecography 18, 200–205.
Rasmussen, S.O., Bigler, M., Blockley, S.P., et al., 2014. A stratigraphic framework for abrupt climatic changes during the Last Glacial period based on three synchronized Greenland ice-core records: refining and extending the INTIMATE event stratigraphy. Quat. Sci. Rev. 106, 14–28.
Reimer, P.J., Bard, E., Bayliss, A., et al., 2013. IntCal13 and Marine13 radiocarbon age calibration curves 0–50,000 years cal BP. Radiocarbon 55, 1869–1887.
Riedinger, M.A., Steinitz-Kannan, M., Last, W.M., Brenner, M., 2002. A 6100 14C yr record of El nino activity from the galapagos islands. J. Paleolimnol. 27, 1–7.
Schiferl, J.D., Bush, M.B., Silman, M.R., 2017. Vegetation responses to late Holocene climate changes in an Andean forest. Quat. Res. 89, 60–74.
Seillès, B., Sánchez Goñi, M.F., Ledru, M.-P., Urrego, D.H., Martinez, P., Hanquiez, V., Schneider, R., 2016. Holocene land–sea climatic links on the equatorial Pacific coast (Bay of Guayaquil, Ecuador). Holocene 26, 567–577.
Stockmarr, J., 1972. Tablets with spores used in absolute pollen analysis. Pollen Spores 13, 615–621.
Svenning, J.-C., 2001a. Environmental heterogeneity, recruitment limitation and the mesoscale distribution of palms in a tropical montane rain forest (Maquipucuna, Ecuador). J. Trop. Ecol. 97–113.
Svenning, J.-C., 2001b. On the role of microenvironmental heterogeneity in the ecology and diversification of neotropical rain-forest palms (Arecaceae). Bot. Rev. 67, 1–53.
Svenning, J.-C., Harlev, D., Sørensen, M.M., Balslev, H., 2009. Topographic and spatial controls of palm species distributions in a montane rain forest, southern Ecuador. Biodivers. Conserv. 18, 219–228.
Svenning, J.C., 1999. Microhabitat specialization in a species-rich palm community in Amazonian Ecuador. J. Ecol. 87, 55–65.
ter Steege, H., Pitman, N.C.A., Sabatier, D., Baraloto, C., et al., 2013. Hyperdominance in the Amazonian Tree Flora. Science 342, 1243092.
Terborgh, J., 1977. Bird species diversity on an Andean elevational gradient. Ecology 58, 1007–1019.
Urrego, D.H., Bush, M.B., Silman, M.R., 2010. A long history of cloud and forest migration from Lake Consuelo, Peru. Quat. Res. 73, 364–373.
Urrego, D.H., Silman, M.R., Correa-Metrio, A., 2011. Pollen–vegetation relationships along steep climatic gradients in western Amazonia. J. Veg. Sci. 22, 795–806.
van Breukelen, M.R., Vonhof, H.B., Hellstrom, J.C., Wester, W.C.G., Kroon, D., 2008. Fossil dripwater in stalagmites reveals Holocene temperature and rainfall variation in Amazonia. Earth Planet Sci. Lett. 275, 54–60.
van Der Werff, H., Consiglio, T., 2004. Distribution and conservation significance of endemic species of flowering plants in Peru. Biodivers. Conserv. 13, 1699–1713.
Veldkamp, J., 2015. Arundinella (Gramineae) in Malesia with notes on other taxa and on aluminium accumulation. Blumea-Biodiversity, Evolution and Biogeography of Plants 59, 167–179.
Weng, C., 2005. An improved method for quantifying sedimentary charcoal via a volume proxy. Holocene 15, 298–301.